Polish Journal of Chemical Technology, 19, 3, 115—119, 10.1515/pjct-2017-0057

PANI/$NaTaO_3$ composite photocatalyst for enhanced hydrogen generation under UV light irradiation

Beata Zielińska[1], Beata Schmidt[2], Ewa Mijowska[1], Ryszard Kaleńczuk[1]

West Pomeranian University of Technology, Szczecin, Faculty of Chemical Technology and Engineering
[1]Nanomaterials Physicochemistry Department
[2]Polymer Institute
[*]Corresponding author: e-mail: bzielinska@zut.edu.pl

A PANI/$NaTaO_3$ composite was successfully synthesized by an oxidative polymerization of aniline monomer in hydrochloric acid solution containing sodium tantalate. $NaTaO_3$ at a monoclinic structure was produced via hydrothermal method. The photocatalytic activities of the unmodified $NaTaO_3$ and PANI/$NaTaO_3$ were evaluated for hydrogen generation from an aqueous HCOOH solution and under UV light irradiation. The results showed that the evolution rate of H_2 increased significantly when $NaTaO_3$ was modified with PANI. The enhancement of the photocatalytic activity of PANI/$NaTaO_3$ composite was ascribed to the effective charge transfer and separation between $NaTaO_3$ and PANI, which reduced their recombination. This indicates that PANI modification of tantalate photocatalysts may open up a new way to prepare highly efficient catalytic materials for H_2 generation.

Keywords: polyaniline, $NaTaO_3$, composite photocatalysts, hydrogen generation.

INTRODUCTION

In the past few decades, a variety of research studies have been performed to develop heterogeneous photocatalysis for the removal toxic organic and inorganic contaminants from aqueous and gas phase and water splitting into hydrogen and oxygen. A wide group of photocatalytic materials which showed high activity for H_2 evolution is tantalates[1–10]. In 1998 Kato and Kudo reported that alkali tantalates such as $LiTaO_3$, $NaTaO_3$ and $KTaO_3$ are efficient photocatalysts for water decomposition into hydrogen and oxygen in the UV region[1]. Thereafter, different tantalate catalysts ($Na_2Ta_2O_6$ $K_2Ta_2O_6$, $CaTa_2O_6$, $SrTa_2O_6$, $BaTa_2O_6$, $Rb_4Ta_6O_{17}$, $Sr_5Ta_4O_{15}$, $Ba_5Ta_4O_{15}$ and $K_3Ta_3B_2O_{12}$) have been studied in the reaction of photocatalytic hydrogen production[4–7]. Moreover, for improvement of the photocatalytic activity of tantalates many different strategies such as metal deposition, doping of metal or non-metal ions or mixing with another oxide have been investigated[8–10].

Conducting polymer composites have received significant attention due to their wide applications in various fields such as charge storage materials, catalysts, solar cells, immunodiagnostic assays and electrorheological ER fluids[11]. Here, many composites of polyaniline (PANI), polypyrrole (Ppy), polyphenylene vinylene (PPV) and polythiophene (PTh) with inorganic compounds ($LiMnO_2$, Pt, Cu, SiO_2, WO_3, Ta_2O_5, MnO_2, TiO_2) have been studied[11–12]. Moreover, both unmodified conducting polymers and conducting polymer nanocomposites can be used as catalysts in the photocatalytic processes. For example, Kandiel et al.[13] reported that TiO_2 modified with Pt-polypyrrole and synthesized via "in situ" simultaneous reduction of Pt(IV) and the oxidative polymerization of Ppy monomers showed enhanced photocatalytic H_2 production activity in respect to Pt-loaded TiO_2. Zhang et al.[14] studied photocatalytic H_2 production from water with Na_2S and Na_2SO_3 as sacrificial reagents and under vis-light irradiation in the presence of PANI/PdS-CdS catalysts. It had been stated that the PANI/PdS-CdS showed high photocatalytic activity for H_2 evolution despite the absence of Pt co-catalyst. Furthermore, the anti-photocorrosion performance of PdS-CdS was also significantly enhanced. Moreover, the PPy/CdS composite materials were investigated to split water under visible-light irradiation[15]. The results showed that for PPy/CdS composite the rate of H_2 evolution was 4.4 times higher than that of unmodified CdS.

In the current study, we report the synthesis of a PANI/$NaTaO_3$ composite photocatalyst via oxidative polymerization of aniline monomer in the presence of $NaTaO_3$. The photocatalytic reaction was carried out in the presence of formic acid as an electron donor and under UV light irradiation. It has been stated that the as-prepared PANI/$NaTaO_3$ exhibited higher activity in the reaction of photocatalytic H_2 generation in comparison to the pristine $NaTaO_3$.

EXPERIMENTAL SECTION

Preparation of $NaTaO_3$

Sodium tantalate ($NaTaO_3$) was prepared by hydrothermal method using Ta_2O_5 (purity 99.99%, Aldrich) and NaOH (purity 98%, Sigma-Aldrich) as precursors. In the first step of the $NaTaO_3$ synthesis, 4 g of Ta_2O_5 was added to 50 cm^3 of aqueous solution of 8M NaOH. Then the solution was sonicated at the room temperature for 1 h. Thereafter, the mixture was poured into Teflon lined stainless steel with a capacity of 70 cm^3. The hydrothermal reaction was carried out at 200°C for 12 h. The final product was collected by filtration, washed with distilled water and dried at 100°C for 48 h.

Preparation of PANI/$NaTaO_3$ composite

PANI/$NaTaO_3$ composite was prepared as follows: 2 g of $NaTaO_3$ was dispersed in the solution that contains 8 ml H_2O and 2 ml HCl. Then aniline monomer (0.1 ml) was added to the above suspension with constant mixing for 1 h. After that the reactor vessel was transferred to an ice bath and the APS ($(NH_4)_2S_2O_8$, 8 cm^3, 0.01 mol/dm^3) was added by dropwise. The obtained mixture was stirred for 2 h. Finally, the sediment was filtrated, washed with water and then dried at 100°C for 48 h.

Experimental procedure and techniques

The morphology of the prepared samples was investigated by high-resolution transmission electron microscopy (HRTEM, Tecnai F30 with a field emission gun operating at 200 kV). The phase composition of the samples was determined using X-ray diffraction analysis (XPert PRO Philips diffractometer, CuK_α radiation). UV-vis diffuse reflectance spectra were recorded using a UV-vis spectrometer (Jasco, Japan). The FTIR spectra were carried out on a Nicolet 308 spectrometer. Photoluminescence (PL) properties at 270 nm excitation of studied materials were studied by using F-7000 Spectrofluorometer (Hitachi).

Photocatalytic reactions

The photocatalytic activities of the obtained $NaTaO_3$ and PANI/$NaTaO_3$ composite in the reaction of H_2 evolution in the presence of formic acid were investigated. The reactions were carried out under atmospheric pressure in a closed system with inner-irradiation-type reactor. A medium pressure mercury lamp (150 W) was used as a light source. In a typical photocatalytic experiment, 300 mg of catalyst was dispersed in 700 cm^3 of 0.1 M aqueous solution of formic acid. Afterwards, the suspension was mixed with a magnetic stirrer for 60 min, and during this time argon was passed through the reaction mixture to remove the dissolved oxygen. Finally, the solution was irradiated for 120 min without argon purging. The evolved hydrogen was collected and analysed by a gas chromatography (Thermal Conductivity Detector (TCD), Ar as a gas carrier, model: Chrome5).

RESULTS AND DISCUSSION

Figure 1 shows the X-ray diffraction patterns of pure PANI, $NaTaO_3$ and PANI/$NaTaO_3$ composite. XRD pattern of PANI shows a week and broad diffraction peaks at 2θ value of 20° and 25°, corresponding to the periodicity parallel to the polymer chains of PANI[16]. The sample obtained after the hydrothermal reaction of NaOH and Ta_2O_5 is composed of sodium tantalate phase at a monoclinic structure ($NaTaO_3$, JCPDS card no 74-2479). For PANI/$NaTaO_3$ composite, only the diffraction peaks of $NaTaO_3$ phase have been detected. The absence of reflections for PANI could be ascribed to the weak crystallinity and small doping content of PANI in composite[16–17].

Figure 2 shows the TEM images of the $NaTaO_3$ and PANI/$NaTaO_3$ composite at different magnifications.

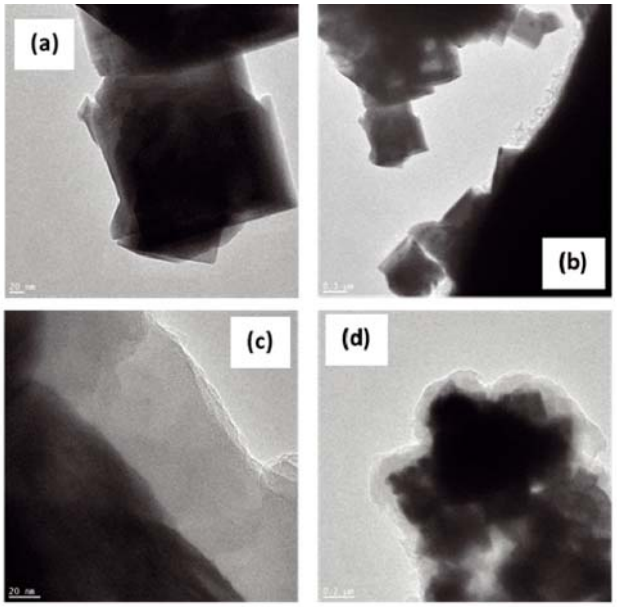

Figure 2. TEM images of samples $NaTaO_3$ (a–b) and PANI/$NaTaO_3$ (c–d)

From TEM images (a–b) it is clearly seen that $NaTaO_3$ shows the well crystallized cubic morphology. From Figure 2 (c–d), it is clearly seen that PANI/$NaTaO_3$ is composed of two phases (c–d) and polyaniline formed a layer on the surface of $NaTaO_3$. The thickness of the PANI layer deposited on $NaTaO_3$ is equal about 80 nm. Moreover, the agglomeration of $NaTaO_3$ particles in the PANI composite was noted (see Fig. 2, image d).

The FTIR transmission spectra of the produced PANI, $NaTaO_3$ and PANI/$NaTaO_3$ composite are shown in Figure 3. The main characteristic bands of pure PANI are assigned as follows: the peaks at 1573 cm^{-1} and 1498 cm^{-1} are attributed to the C=N and C=C stretch-

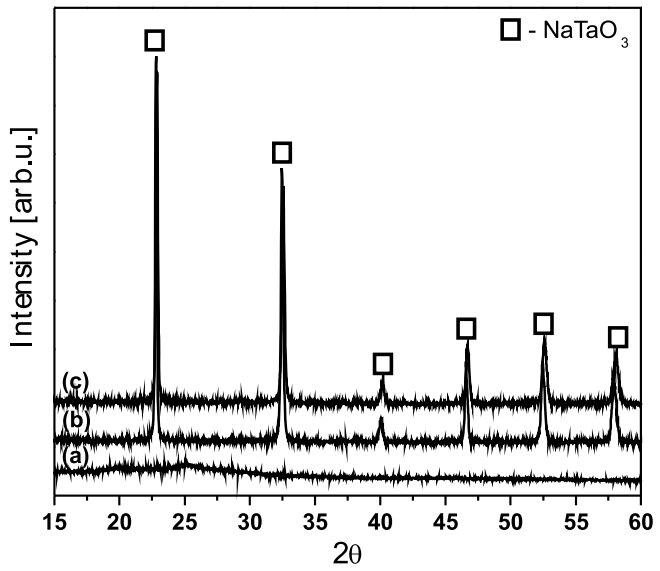

Figure 1. A comparison of X-ray diffraction patterns of samples: (a) PANI, (b) $NaTaO_3$ and (c) PANI/$NaTaO_3$

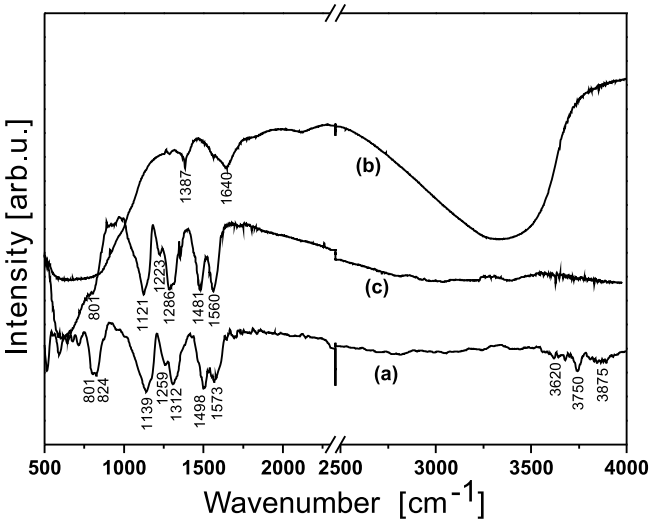

Figure 3. FTIR/DRS spectra of (a) PANI, (b) $NaTaO_3$ and (c) PANI/$NaTaO_3$

ing modes of the quinonoid and benzenoid rings, the bands at 1259 cm^{-1} and 1255 cm^{-1} are assigned to C-N stretching mode for benzenoid units, while the peak at 798 cm^{-1} is associated with C-C and C-H for benzenoid units[17–20]. Otherwise, the broad and sharp peaks in the range of 3419–3508 cm^{-1} are attributed to N-H stretching vibration[18]. The FTIR spectrum of $NaTaO_3$ shows bands at 1387 cm^{-1}, 1630 cm^{-1}, a broad band in the region of 2600–3600 cm^{-1} and a broad band in the range of 500–1200 cm^{-1}. A broad and strong peak in the range of 2600–3600 cm^{-1} and a peak at 1630 cm^{-1} are assigned to the bending of O-H-O and stretching of O-H modes due to the presence of physically adsorbed water on the surface of the samples[21]. The bands between 500–1200 cm^{-1} and at 1387 cm^{-1} correspond to the Ta-O and Na-O vibrations, respectively[22]. The FTIR spectrum of PANI/$NaTaO_3$ composite shows seven peaks at about 783 cm^{-1}, 1144 cm^{-1}, 1310 cm^{-1}, 1500 cm^{-1}, 1588 cm^{-1}, 3230 cm^{-1} and 3450 cm^{-1}. All those peaks are characteristic bands of PANI and confirmed the presence of PANI in the synthesized composite. Moreover, for PANI/$NaTaO_3$ composite all characteristic peaks of PANI shifted to the lower wavenumber in comparison to the pure PANI. This effect can be explained by the strong interaction between PANI and $NaTaO_3$ in the composite.

TGA curves of PANI and PANI/$NaTaO_3$ composite are shown in Figure 4. For both samples two steps of weight loss are observed. The first weight loss (25–120°C) of about 12% for PANI and 3% for PANI/$NaTaO_3$ is due to the removal of water adsorbed on the surface of the samples. The second significant weight reduction (330–600°C) is attributed to the polymer backbone decomposition[23]. Moreover, according to the data from TG analysis, it was found that the content of PANI in PANI/$NaTaO_3$ composite is about 30 wt%.

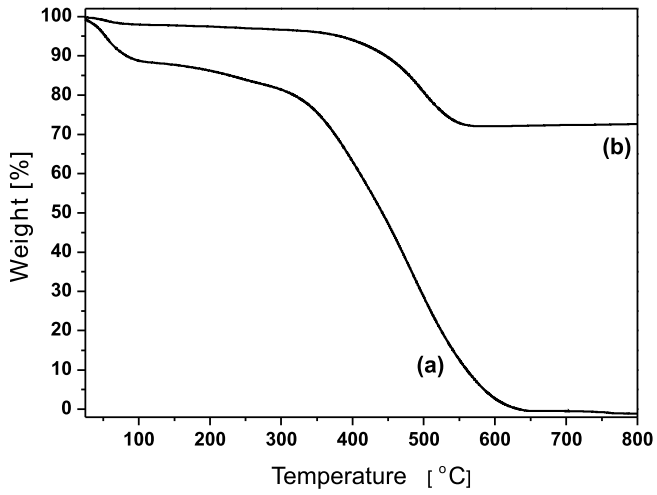

Figure 4. TGA profiles of PANI (a) and PANI/$NaTaO_3$ (b) samples

Figure 5 shows a comparison of UV-vis absorbance spectra of PANI, $NaTaO_3$ and PANI/$NaTaO_3$ composite. The spectrum of PANI shows two strong peaks. The peak at about 320 nm is assigned to the π-π * transition of benzene rings and the peak at about 630 nm is attributed to the transition of the quinoid rings in long PANI chains[20]. For pure $NaTaO_3$ a single absorption edge at around 300 nm, indicating the band gap energy of 4.11eV

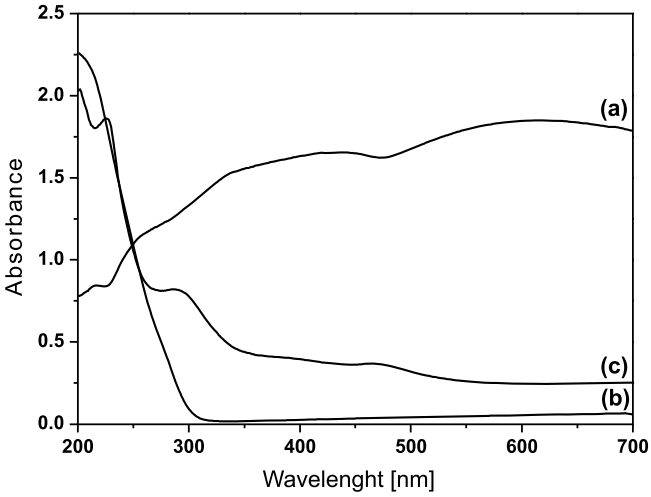

Figure 5. DR-UV-vis spectra of (a) PANI, (b) $NaTaO_3$ and (c) PANI/$NaTaO_3$

can be observed. The estimated band gap of unmodified $NaTaO_3$ is similar to that described in literature[24, 25]. Moreover, it can be noted that the characteristic bands of both polyaniline and $NaTaO_3$ have been observed for PANI/$NaTaO_3$ composite. Here, a clear agreement with XRD, TEM and FTIR data is demonstrated.

The photocatalytic H_2 production studies under UV light irradiation were evaluated over unmodified $NaTaO_3$ and PANI/$NaTaO_3$ composite using HCOOH as an electron donor. The control reactions without HCOOH have been also investigated. Here, a trace amount of H_2 was observed in these reaction conditions for both unmodified and modified $NaTaO_3$. The results of hydrogen evolution are presented in Figure 6. Here, one can notice that PANI/$NaTaO_3$ exhibits higher photocatalytic activity than unmodified $NaTaO_3$. It indicates that polyaniline plays a crucial role in the photocatalytic reaction. Also, the reaction of photocatalytic H_2 evolution during the first 120 min of UV light irradiation can be described by zero order kinetics. The rate constants of H_2 evolution are about 87 μmol/h and 163 μmol/h for $NaTaO_3$ and PANI/$NaTaO_3$, respectively. It is known that the result of a photocatalytic reaction depends mainly on separation, mobility and the lifetime of photogenerated electrons and holes. Here, the photoluminescence (PL) analysis was used to study the efficiency of electron–hole

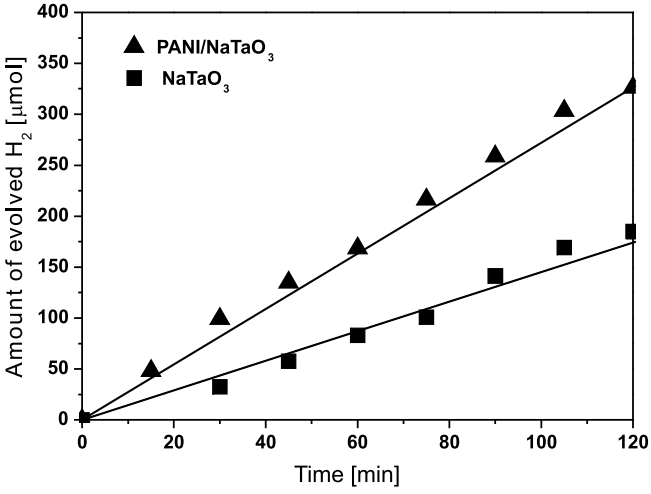

Figure 6. Photocatalytic H_2 evolution over $NaTaO_3$ and PANI/$NaTaO_3$ catalysts

carriers separation and transfer in semiconductors[26–28] and to understand why the introduction of PANI leads to the enhance the photoactivity of $NaTaO_3$. Figure 7 presents the PL emission spectra of PANI, $NaTaO_3$ and PANI/$NaTaO_3$ composite. PANI shows a broad spectrum with low PL intensity. The PL response for $NaTaO_3$ exhibits a strong and broad emission band in the range of 370–500 nm with a maximum at about 420 nm[29–30]. Moreover, it is found that PL spectrum of the PANI/$NaTaO_3$ composite in the same range of wavelength is much lower than that of pure $NaTaO_3$. This results indicated that the recombination of photogenerated electrons and holes was effectively inhibited in the PANI/$NaTaO_3$ composite[26–30]. It suggests that the higher photocatalytic activity of PANI/$NaTaO_3$ can be explained by efficient separation of electrons and holes between those two phases, reducing their recombination.

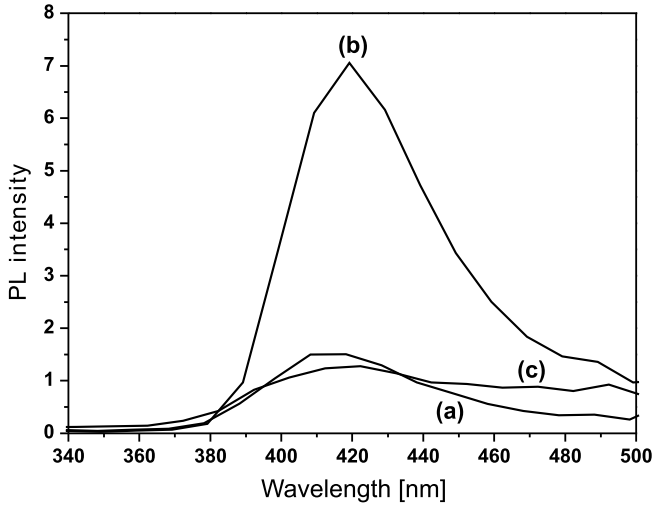

Figure 7. Photoluminescence spectra (a) PANI, (b) $NaTaO_3$ and (c) PANI/$NaTaO_3$

CONCLUSION

In summary, PANI/$NaTaO_3$ composite was successfully prepared via oxidative polymerization of aniline monomer in the presence of $NaTaO_3$. A detailed analysis (TEM, XRD, FTIR, TGA and DR-UV-vis) indicated that PANI formed the layer on the surface of $NaTaO_3$. The photocatalytic properties of the synthesized samples were evaluated for the reaction of photocatalytic H_2 production. It was found that, PANI/$NaTaO_3$ composite exhibited significantly higher photocatalytic activity in respect to the unmodified $NaTaO_3$. The improvement of photocatalytic performance of PANI/$NaTaO_3$ composite was attributed to the efficient photogenerated electron–hole transfer and separation.

LITERATURE CITED

1. Kato, H. & Kudo, A. (1998). New tantalate photocatalysts for water decomposition into H_2 and O_2. *Chem. Phys. Lett.* 295, 487–492.

2. Ikeda, S., Fubuki, M., Takahara, Y.K. & Matsumura, M. (2006). Photocatalytic activity of hydrothermally synthesized tantalate pyrochlores for overall water splitting. *Appl. Catal. A* 300, 186–190. DOI: 10.1063/1.4928288.

3. Kato, H. & Kudo, A. (1999). Photocatalytic decomposition of pure water into H_2 and O_2 over $SrTa_2O_6$ prepared by a flux method. *Chem. Lett.* 28, 1207–1208. DOI: 10.1246/cl.1999.1207.

4. Sayama, K., Arakawa, H. & Domen, K. (1996). Photocatalytic water splitting on nickel intercalated $A_4Ta_xNb_{6-x}O_{17}$ (A=K, Rb). *Catal. Today* 28, 175–182.

5. Yoshioka, K., Petrykin, V., Kakihana, M., Kato, H. & Kudo, A. (2005). The relationship between photocatalytic activity and crystal structure in strontium tantalates. *J. Catal.* 232, 102–107. DOI: 10.1016/j.jcat.2005.02.021.

6. Otsuka, H., Kim, K., Kouzu, A., Takimoto, I., Fujimori, H., Sakata, Y., Imamura, H., Matsumoto, T. & Toda, K. (2005). Photocatalytic performance of $Ba_5Ta_4O_{15}$ to decomposition of H_2O into H_2 and O_2. *Chem. Lett.* 34, 822–823. DOI: 10.1246/cl.2005.822.

7. Kurihara, T., Okutomi, H., Miseki, Y., Kato, H. & Kudo, A. (2006). Highly efficient water splitting over $K_3Ta_3B_2O_{12}$ photocatalyst without loading co-catalyst. *Chem. Lett.* 35, 274–275. DOI: 10.1246/cl.2006.274.

8. Ishihara, T., Nishiguchi, H., Fukamachi, K. & Takita, Y. (1999). Effects of acceptor doping to $KTaO_3$ on photocatalytic decomposition of pure H_2O. *J. Phys. Chem. B.* 103, 1–3.

9. Kudo, A. & Kato, H. (2000). Effect of lanthanide-doping into $NaTaO_3$ photocatalysts for efficient water splitting. *Chem. Phys. Lett.* 331, 373–377. DOI: 10.1016/S0009-2614(00)01220-3.

10. Iwase, A., Kato, H. & Kudo, A. (2009). The effect of alkaline earth metal ion dopants on photocatalytic water splitting by $NaTaO_3$ powder. *Chem. Sus. Chem.* 2, 873–877. DOI: 10.1002/cssc.200900160.

11. Mukthaa, B., Mahantaa, D., Patila, S. & Madras, G. (2007). Synthesis and photocatalytic activity of poly(3-hexylthiophene)/TiO_2 composites. *J. Solid State Chem*. 180, 2986–2989. DOI: 10.1016/j.jssc.2007.07.017.

12. Gangopadhyay, R. & De, A. (2000). Conducting polymer nanocomposites: A brief overview. *Chem. Mater.* 12, 608–622. DOI: 10.1021/cm990537f.

13. Kandiel, T.A., Dillert, R. & Bahnemann, D.W. (2009). Enhanced photocatalytic production of molecular hydrogen on TiO_2 modified with Pt-polypyrrole nanocomposites. *Photochem. Photobiol. Sci.* 8, 683–690. DOI: 10.1039/b817456c.

14. Zhang, S., Chen, Q., Jing, D., Wang, Y. & Guo, L. (2012). Visible photoactivity and antiphotocorrosion performance of PdS-CdS photocatalysts modified by polyaniline. *Int. J. Hydrogen. Energy* 37, 791–796. DOI: 10.1016/j.ijhydene.2011.04.060.

15. Zhang, S., Chen, Q., Wang, Y. & Guo, L. (2012). Synthesis and photoactivity of CdS photocatalysts modified by polypyrrole. *Int. J. Hydrogen Energy* 37, 13030–13036. DOI: 10.1016/j.ijhydene.2012.05.060.

16. Ge, L., Han, C. & Liu, J. (2012). *In situ* synthesis and enhanced visible light photocatalytic activities of novel PANI–g-C_3N_4 composite photocatalysts. *J. Mater. Chem.* 22, 11843–11850. DOI: 10.1039/C2JM16241E.

17. Radocici, M., Saponjic, Z., Jankovic, I.A., Ciric-Marjanovic, G., Ahrenkiel, S.P. & Comor, M.I. (2013). Improvements to the photocatalytic efficiency of polyaniline modified TiO_2 nanoparticles. *Appl. Catal. B* 136–137, 133–139. DOI: 0.1016/j.apcatb.2013.01.007.

18. Wei, J., Zhang, Q., Liu, Y., Xiong, R., Pan, C. & Shi, J. (2011). Synthesis and photocatalytic activity of polyaniline–TiO_2 composites with bionic nanopapilla structure. *J. Nanopart. Res.* 13, 3157–3165. DOI: 10.1007/s11051-010-0212-z.

19. Gao, J., Li, S., Yang, W., Ni, G. & Bo, L.J. (2007). Synthesis of PANI/TiO_2–Fe^{3+} nanocomposite and its photocatalytic property. *Mater. Sci.* 42, 3190–3196. DOI: 0.1007/s10853-006-1353-4.

20. Yavuz, A.G. & Gök, A. (2007). Preparation of TiO_2/PANI composites in the presence of surfactants and investigation of electrical properties. Synth. Metals 157, 235–242. DOI: 10.1016/j.synthmet.2007.03.001.

21. Mozia, S., Tomaszewska, M., Kosowska, B., Grzmil, B., Morawski, A.W. & Kałucki, K. (2005). Decomposition of

nonionic surfactant on a nitrogen-doped photocatalyst under visible-light irradiation. *Appl. Catal. B* 55, 195–200. DOI: 10.1016/j.apcatb.2004.09.019.

22. Li, F.F., Liu, D.R., Gao, G.M., Xue, B. & Jiang, Y.S. (2015). Improved visible-light photocatalytic activity of $NaTaO_3$ with perovskite-like structure via sulfur anion doping. Appl. Catal. B 166–167, 104–111. DOI: 10.1016/j.apcatb.2014.10.049.

23. Yang, J., Wang, X., Wang, X., Jia, R. & Huang, J. (2010). Preparation of highly conductive CNTs/polyaniline composites through plasma pretreating and in-situ polymerization. J. Phys. Chem. Sol. 71, 448–452. DOI: 10.1016/j.jpcs.2009.12.008.

24. Lin, W.H. (2006). $NaTaO_3$ photocatalysts of different crystalline structures for water splitting into H_2 and O_2. Appl. Phys. Lett. 89, 211904. DOI: 10.1063/1.2396930.

25. Lan, N.T., Phan, L.G., Hoang, L.H., Huan, B.D., Hong, L.V., Anh, T.X. & Chinh, N. (2016). Hydrothermal Synthesis, Structure and Photocatalytic Properties of La/Bi Co-Doped $NaTaO_3$. *Mater. Trans*. 57(1), 1–4. DOI: 10.2320/matertrans. MA201517.

26. Wan,g Q., Lian, J., Li, J., Wang, R., Huang, H., Su, B. & Lei, Z. (2015). Highly efficient photocatalytic hydrogen production of flower-like cadmium sulfide decorated by histidine. *Sci. Rep.* 5, 13593–1396. DOI: 10.1038/srep13593.

27. Ansari, M.O., Khan, M.M., Ansari, S.A., Lee, J. & Cho, M.H. (2014). Enhanced thermoelectric behavior and visible light activity of Ag@TiO_2/polyaniline nanocomposite synthesized by biogenic-chemical route. *RSC Adv.* 4, 23713–23719. DOI: 10.1039/c4ra02602k.

28. Xing, Z., Chen, Z., Zong, X. & Wang, L. (2014). A new type of carbon nitride-based polymer composite for enhanced photocatalytic hydrogen production. *Chem. Commun.* 50, 6762–6764. DOI: 10.1039/c4cc00397g.

29. Kato, H. & Kudo, A. (2001). Water splitting into H_2 and O_2 on alkali tantalate photocatalysts $ATaO_3$ (A = Li, Na, and K). *J. Phys. Chem. B* 105, 4285–4292. DOI: 10.1021/jp004386b.

30. Hu, C.C., Tsai, C.C. & Teng, H. (2009). Structure characterization and tuning of perovskite-like $NaTaO_3$ for applications in photoluminescence and photocatalysis. *J. Am. Ceram. Soc.* 92(2), 460–466. DOI: 10.1111/j.1551-2916.2008.02869.x.